Supplementary Informatin

Identification of a nano-abzyme able to catalyze the destruction of the spike-trimer of SARS-CoV-2

Kai Wang[1#], Duanfang Cao[2#], Lanlan Liu[1,3#], Xiaoyi Fan[2,3#], Yihuan Lin[1], Wenting He[2,3], Yunze Zhai[4], Pingyong Xu[2,3], Xiyun Yan[2,3], Haikun Wang[4*], Xinzheng Zhang[2,3*], Pengyuan Yang (✉)[1,3,5]

[1] Key Laboratory of Epigenetic Regulation and Intervention, Institute of Biophysics, Chinese Academy of Sciences, Beijing 100101, China.

[2]National Laboratory of Biomacromolecules, CAS Center for Excellence in Biomacromolecules, Institute of Biophysics, Chinese Academy of Sciences, Beijing 100101, China.

[3]University of Chinese Academy of Sciences, Beijing 100049, China.

[4]State Key Laboratory of Cardiology and Medical Innovation Center, Shanghai East Hospital, School of Medicine, Tongji University, Shanghai 200120, China.

[5]Lead contact

✉Corresponding: hkwang@tongji.edu.cn (H.W), xzzhang@ibp.ac.cn (Z.Z), pyyang@ibp.ac.cn (P.Y)

[#]These authors contributed equally to this work.

Supplementary Figures

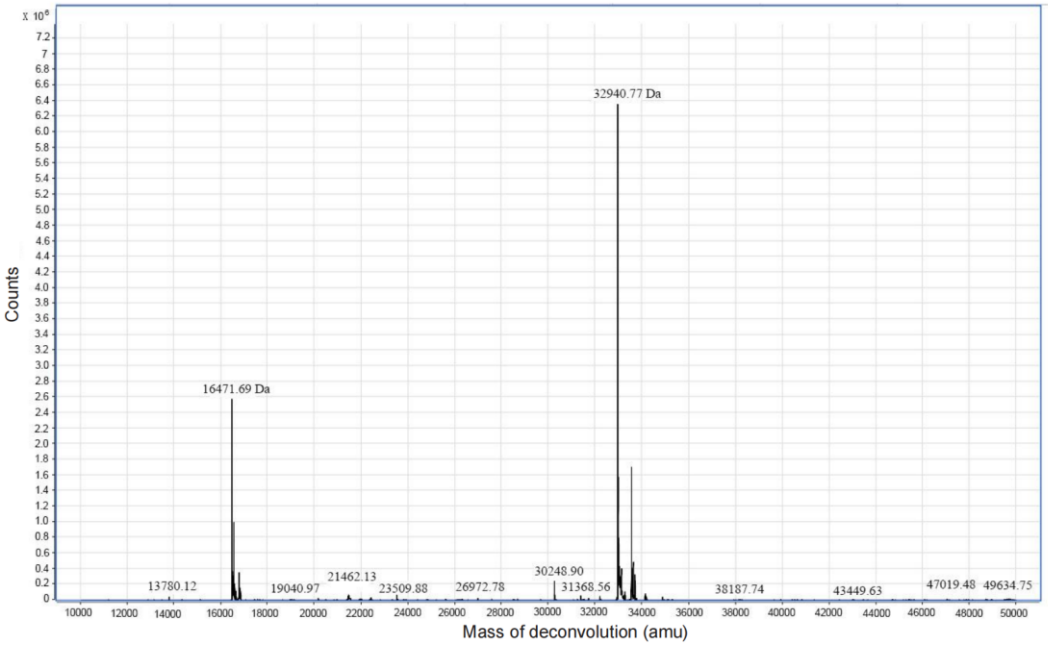

Fig. S1. Characteristics of immune serums, VHH library and candidate VHHs. **(A)** The levels of 6000 times diluted serums against WT S protein after immunization were detected through ELISA. Pre-immunization serum was used as a negative control. Data are mean ± SD of three independent experiments. **(B-C)** Binding capacity assay of the 5th immunization serum of male camel that was 3-fold serial dilutions were detected through ELISA, Data are mean ± SD of three independent experiments. **(D)** The VHH fragments were specifically amplified by PCR, and the mock was the control without template. **(E)** The VHH fragments were inserted into pComb3xSS vector by electric transfer, and the insertion rate was detected by colony-PCR. The vector without electric transfer was used as negative control. **(F)** Bar graph were detected through phage ELISA and showing the binding capacity of VHH candidates screened by biopanning. Data are mean ± SD of three independent experiments. **(G)** Heat maps showing the binding capacity assay of six VHHs to S1 proteins of SARS-CoV-2 VOCs, SARS-CoV, BatRaTG13, MERS-CoV and hCoV-229E by competitive ELISA. **(H)** Binding capacity assays of five other

VHH candidates, performed using VHH ELISA, showing cross-reactivity to the S1 proteins mentioned above. Datapoints represent the mean ± SD of three independent experiments. **(I)** The average distance tree of nanobody candidates identified by phage display, calculated by percentage identity. **(J)** ClustalW alignment of the amino-acid sequences of VHHs. The CDR regions are marked with horizontal lines.

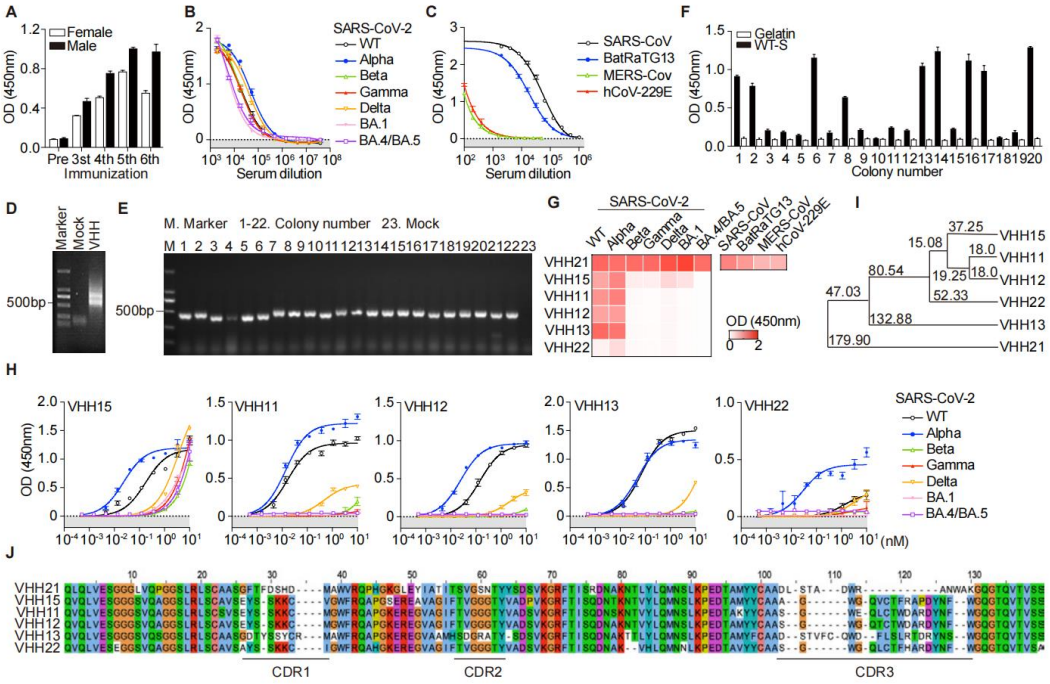

Fig. S2. The deconvoluted ESI-MS spectrum of the VHH 21, related to STAR Methods: Mass spectrum

Three μL of VHH21 sample was loaded into the HPLC column and separated using a 2-98% linear gradient in 10 min with a flow rate of 0.2 mL/min. The graph shows that the the two peaks at the positions of the molecular mass of 16471.69 Da and 32940.77 Da correspond to the monomeric and dimeric VHH21, respectively.

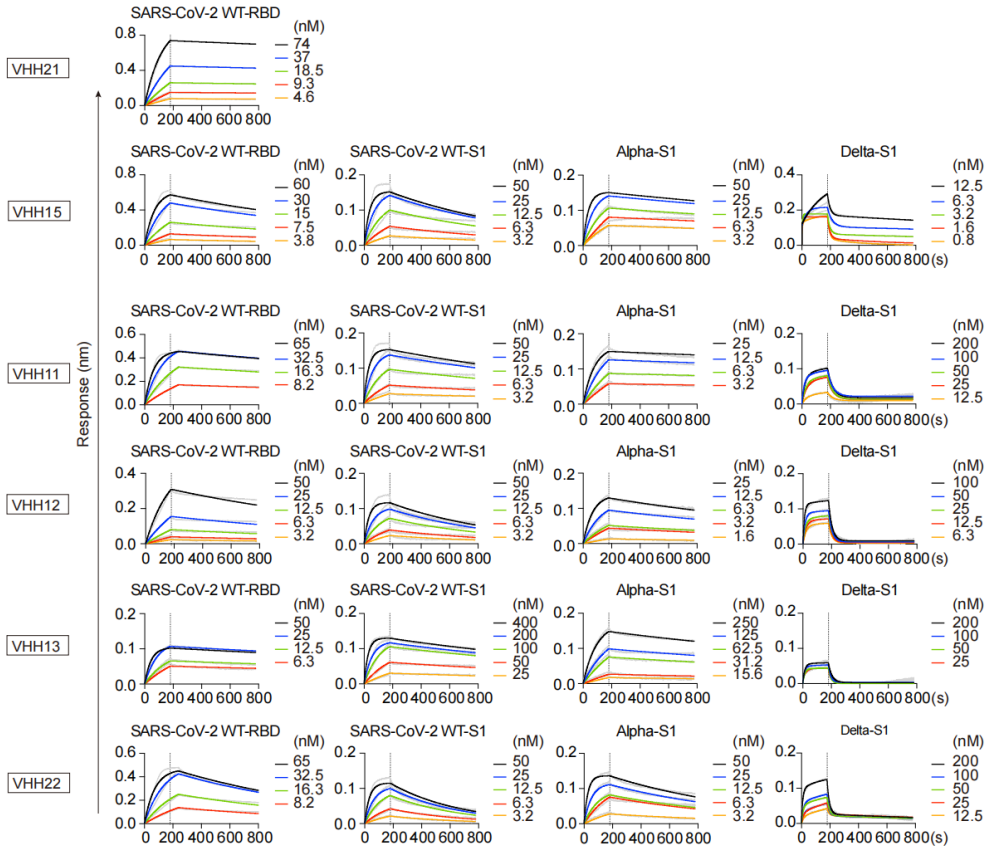

Fig. S3. VHHs binding kinetics to SARS-CoV-2 WT RBD and VOCs S1 proteins.

SARS-CoV-2 S1 proteins of different variants and RBD proteins were immobilized on Octet SA sensors as in Fig. 1c and a dilution series nanobodies were association for 180 s, followed by dissociation for 600 s. grey trace represents the raw data, and colored lines. Dissociation constants (K_D) show in table S2 were determined on the basis of fits, applying a 1:1 interaction model. Representative binding curves are shown from three independent experiments.

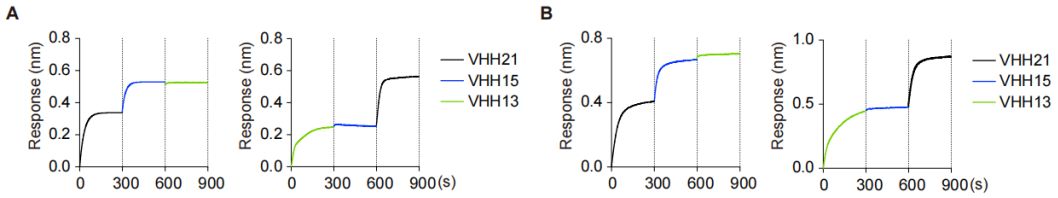

Fig. S4. BLI response analysis of VHHs competition binding to SAR-CoV-2 VOCs S1 proteins.

(A-B) 15 μg/mL biotinylated WT **(A)** and alpha **(B)** S1 proteins were immobilized on Octet SA sensors, respectively. Followed binding to VHHs one by one, apiece association for 300 s, without dissociation process. Representative binding curves are shown from three independent experiments.

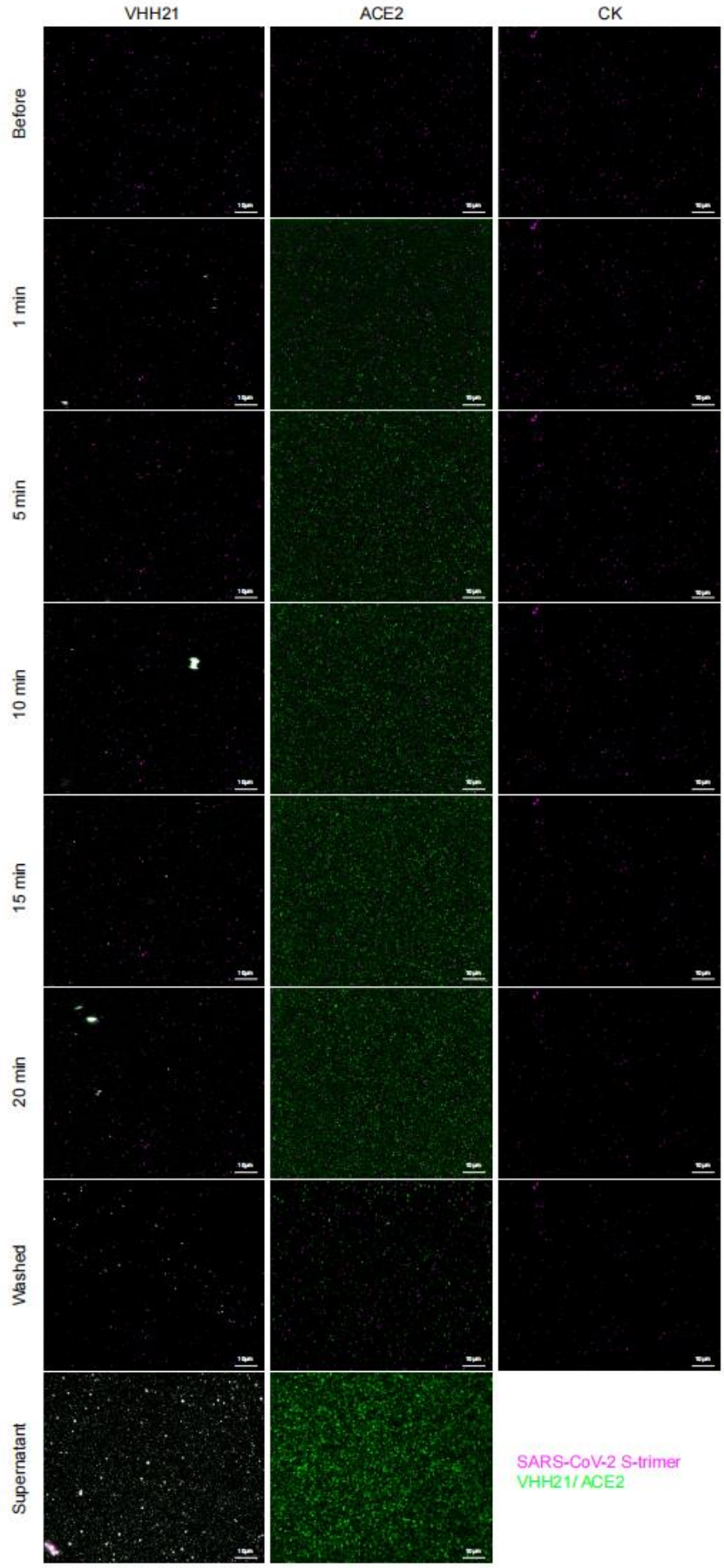
VHH21
ACE2
CK
Before
1 min
5 min
10 min
15 min
20 min
Washed
Supernatant
SARS-CoV-2 S-trimer
VHH21/ ACE2

Fig. S5. Original size confocal images showed in Figure 3D in all time points. Immobilized staining S-trimer complexes (light purple) were treated with staining VHH21 complexes (green). Treated with PBS buffer and staining ACE2 complexes (green) were as CK and control group, respectively. Confocal images (Pixel size:100nm) were recorded before (not added staining VHH or ACE2 complexes) and every 1 min for 20 minutes, the washed bottom of the plate and the supernatant of added staining VHH or ACE2 complexes transferred to a new empty well. The images were collected and representative images are from three independent experiments. Scale bars, 10 μm.

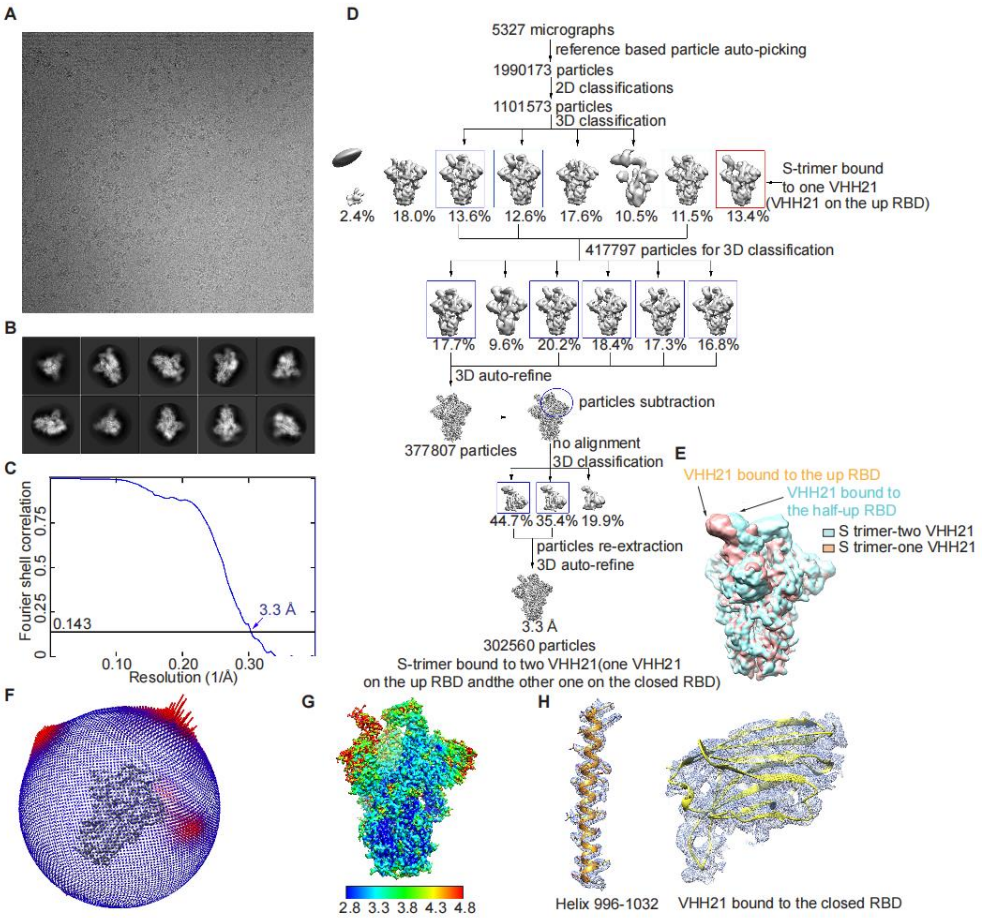

Fig. S6. Cryo-EM data analysis of the complex of SARS-CoV-2 S-trimer and VHH21.

(A) Representative cryo-EM micrograph of the complex of SARS-CoV-2 S-trimer and VHH21. **(B)** Representative 2D class averages. **(C)** Gold-standard Fourier shell correlation (FSC) curves. **(D)** Cryo-EM data processing workflow. **(E)** Comparison of the density maps of S-trimer bound to two VHH21 (light blue) and S-trimer bound to one VHH21 (light orange) with the opened RBD in half-up and up conformations. **(F)** Orientational distribution of the particles in the final 3D auto-refinement. **(G)** Local resolution estimates of the density map. **(H)** Representative cryo-EM densities of the central helix (left) and the VHH21 bound to the closed RBD (right).

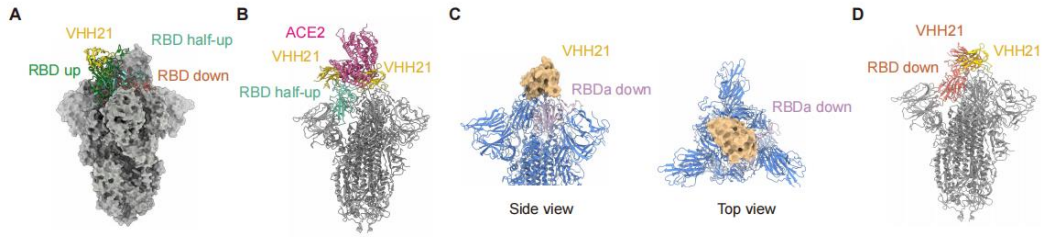

Fig. S7. VHH21 bind to different epitopes and perfectly avoid RBD mutation sites.

(A-C) Structural analysis of different structures superposed onto S-trimer in complex with VHH21. **(A)** Comparison of RBD in down (salmon, PDB: 6Z97), totally up (forest green, PDB: 6ZGI) and half-up comformation from our structure (aquamarine). **(B)** Superposition of ACE2-bound RBD (hot pink, PDB: 6M0J) to half-up RBD from our structure. **(C)** Structure superposition of VHH21-bound RBD to the RBD from all closed S-trimer. Diagram of side and top views for structure superposition of VHH21-bound RBD to the RBDa (thistle) from all closed S trimer (cornflower blue, PDB: 6ZGI). VHH21 is shown as surface mode. **(D)** We replaced the VHH21-bound half-up RBD in our structure with a VHH21-bound down RBD (salmon).

Supplementary Movie

Movie S1. VHH21 bind and destruct the S-trimer of SARS-CoV-2 compared with ACE2 (STED).

The staining S-trimer complexes (light purple) unevenly immobilized on the bottom of the wells. Once staining VHH21or ACE2 complexes (green) were added, microscopy images were recorded 1 image per sec for 20 minutes at room temperature (Scale bar: 10 μm).

Movie S2. VHH21 bind and destruct the S-trimer of SARS-CoV-2 compared with ACD2 (TIRF).

The staining S-trimer complexes (light purple) unevenly immobilized on the bottom of the wells. Once the images beginning to record, the staining VHH21or ACE2 complexes (green) were added, microscopy images were recorded 20 image per sec for 100 seconds at room temperature (Scale bar: 5 μm).

Supplementary Tables

Table S1. Cryo-EM data collection, refinement and validation statistics

	SARS-CoV-2 S/VHH21 (EMDB 33510) (PDB 7XY4)
Data collection and processing	
Magnification	130,000
Voltage (kV)	300
Electron exposure (e–/Å^2)	60
Defocus range (μm)	1.8-2.2
Pixel size (Å)	1.04
Symmetry imposed	C1
Initial particle images (no.)	1,990,173
Final particle images (no.)	302,560
Map resolution (Å)	3.3
FSC threshold	0.143
Map resolution range (Å)	2.8-4.8
Refinement	
Initial model used (PDB code)	7DK3
Model resolution (Å)	
FSC threshold	0.5
Model resolution range (Å)	2.8-4.8
Map sharpening *B* factor (Å^2)	-146
Model composition	

Non-hydrogen atoms	27,307
Protein residues	3,422
Ligands	41
B factors (Å^2)	
Protein	87
Ligand	88
R.m.s. deviations	
Bond lengths (Å)	0.01
Bond angles (°)	1.17
Validation	
MolProbity score	1.71
Clashscore	4.90
Poor rotamers (%)	0.03
Ramachandran plot	
Favored (%)	92.93
Allowed (%)	7.07
Disallowed (%)	0

129

130

Table S2. Summary of information about VHH libraries

Library	Library size (cfu)	Insert rate (%)	Correct rate (%)	Phage titer (pfu/ml)
A	1.04×10^{8}	100	100	4.4×10^{11}
B	1.98×10^{8}	100	100	1.53×10^{12}

133 **Table S3. Summary of kinetic rate and equilibrium dissociation constants**

	SARS-CoV-2 WT RBD	SARS-CoV-2 WT S1	Alpha S1	Beta S1	Gamma S1	Delta S1	BA.1/ BA.2 S1	BA.4/ BA.5 S1
K_D								
VHH 21	0.82	0.37	0.32	0.99	0.52	0.69	2.96	7.89
VHH 15	2.47	1.91	0.51	ND	ND	0.44	ND	ND
VHH 11	1.02	0.88	0.43	ND	ND	3.88	ND	ND
VHH 12	3.56	2.23	0.76	ND	ND	45.04	ND	ND
VHH 22	4.10	3.62	1.10	ND	ND	1.28	ND	ND
VHH 13	0.94	5.28	13.60	ND	ND	1.38	ND	ND
K_d ($\times 10^4 s^{-1}$)								
VHH 21	0.93	0.95	1.00	3.18	2.17	4.20	4.66	10.52
VHH 15	5.75	9.92	2.78	ND	ND	8.5	ND	ND
VHH 11	2.50	5.09	2.65	ND	ND	65.78	ND	ND
VHH 12	5.69	12.88	4.33	ND	ND	289.90	ND	ND
VHH 22	8.19	20.04	8.44	ND	ND	42.50	ND	ND
VHH 13	3.64	4.64	3.47	ND	ND	0.91	ND	ND
K_a ($\times 10^{-4} M^{-1} s^{-1}$)								
VHH 21	1.14	2.54	3.13	3.20	4.21	6.10	3.04	13.34
VHH 15	2.33	5.19	5.46	ND	ND	19.35	ND	ND
VHH 11	2.46	5.81	6.20	ND	ND	16.95	ND	ND
VHH 12	1.60	5.78	5.67	ND	ND	6.44	ND	ND

VHH 22	2.00	5.54	7.68	ND	ND	33.26	ND	ND
VHH 13	3.89	0.88	0.26	ND	ND	0.07	ND	ND

ND: Not detectable due to response < 0.05.

136 **Table S4**

Reagent or Resource	SOURCE	IDENTIFIER
Proteins		
SARS-CoV-2 RBD-His-tag	Sino Biological	40589-V08H
SARS-CoV-2 RBD-mFc-tag	Sino Biological	40592-V05H
SARS-CoV-2 RBD-AVI & his-tag	Sino Biological	40592-V27H-B
SARS-CoV-2 S1+S2-His-tag	Sino Biological	40589-V08B1
SARS-CoV-2 S1- mFc-tag	Sino Biological	40591-V05H1
SARS-CoV-2 S1-AVI & his-tag	Sino Biological	40591-V27H-B
SARS-CoV-2 S1(D614G) -his-tag	Sino Biological	40591-V08H3
B.1.17(Alpha) S1-His-tag	Sino Biological	40591-V08H12
B.1.351 (Beta) S1-His-tag	Sino Biological	40591-V08H15
P.1 (Gamma) S1-His-tag	Sino Biological	40591-V08H14
B.1.617.2 (Delta) S1-His-tag	Sino Biological	40591-V08H23
B.1.1.529 (BA.1) S1-His-tag	Sino Biological	40591-V08H41
BA.4/BA.5 S1-His-tag	Sino Biological	40591-V08H46
SARS-CoV-1 S1-His-tag	Sino Biological	40150-V08B1
BatCoV-RaTG13 S1-His-tag	R&B SYSTEMS	10662-CV-100
MERS-CoV S1-His-tag	Sino Biological	40069-V08H
hCoV-229E S1-His-tag	Sino Biological	40601-V08H
ACE2-His-tag	Sino Biological	10108-H08H
SARS-CoV-2 S-His-tag	This paper	N/A
SARS-CoV-2 S-mutant-His tag	This paper	N/A
Antibodies		

Mouse anti His-tag antibody	ABClonal	AE003
Mouse anti His-tag-HRP antibody	Proteintech	HRP-66005
Rabbit anti NTD antibody	GeneTex	GTX635656
Mouse anti S2 antibody	GeneTex	GTX632604
Goat anti rabbit-HRP antibody	ZSGB-BIO	ZB2301
Alexa Fluor 555-labeled donkey anti-rabbit antibody	Beyotime	A0453
Alexa Fluor488-labeled goat anti-mouse antibody	Beyotime	A0428
Abberiors STAR RED goat anti rabbit antibody	Abberior	10324PK-3
Abberiors STAR ORANGE goat anti mouse antibody	Abberior	10324PK-2
Rat anti HA-tag-HRP antibody	Roche	12013819001
Rabbit anti fd bacteriophage antibody	Sigma-Aldrich	B7786-.2ml
Rabbit anti llama antibody	Invitrogen™	A16154
Cells		
TOP10 cells	Biomed	BC101-2
DH10BAC cells	Biomed	BC112-01
Sf21 Cells	Gibco™	11497-013
High Five™ Cells	Gibco™	B85502
TOP10F´ cells	Invitrogen™	C66511
ER2738 cells	Lucigen	60522-1
M13KO7 helper phage	NEB	N0315S
293T-ACE2 cells	Provided by Haikun Wang	N/A
Chemicals and other		
Complete Freund’ s adjuvant	Sigma-Aldrich	F5881-10ML

incomplete Freund's adjuvant	Sigma-Aldrich	F5506-10ML
Bovine serum Albumin	Sigma-Aldrich	V900933
Gelatin from porcine skin	Sigma-Aldrich	48722-500G-F
Thrombin	Sigma-Aldrich	T4648
Glutaraldehyde solution	Sigma-Aldrich	G6257-10mL
Assay plate, 96 Well	Costar®	3922
Microtiter plate, 96 Well	Costar®	2592
96 Well glass bottom plate, 96 Well	Cellvis	P96-1.5H-N
Streptavidin (SA) Biosensors	Fortebio	18-5019
Streptavidin Coated 96-Well Plate	Beaver	22351
Isopropyl β-d-1-thiogalactopyranoside	Solarbio	I8070
M13KO7 helper phage	NEB	N0315S
Sfi I Restriction Endonucleases	NEB	R0123L
T4 DNA Ligase	NEB	M0202L
Furin	NEB	P8077L
DpnI	NEB	R0176V
SF-900™ II SFM	Gibco™	10902104
Cellfectin™ II Reagent	Gibco™	10362100
Fetal Bovine Serum	Gibco™	10270-106
HisPur™ Ni-NTA Resin	Thermo Scientific™	88223
GIG Holey carbon grids	EMCN	GiG-10104C
Golden®StarT6 Super PCR Mix (1.1×)	TSINGKE	TSE101
Critical Commercial Assays		
LeukoLOCK™ Total RNA Isolation System	Invitrogen™	AM1923

Bright-Glo™ Luciferase Assay System	Promega	E2620
PrimeScript™ II 1st Strand cDNA Synthesis Kit	TaKaRa	6210A
QIAquick Gel Extraction Kit	QIAGEN	28704
QIAquick PCR Purification Kit	QIAGEN	28104
TIANprep Mini Plasmid Kit	TIANGEN	DP103-02
Biotinylation Kit	Genemore	G-MM-IGT

Primers

GSP-RT: CGCCATCAATRTACCAGTTGA

LP-leader: GTGGTCCTGGCTGCTCTW

VH-F1: CATGCCATGACTGTGGCCCAGGCGGCCCAGKTGCAGCTCGTGGAGTC

VHH-R3: CATGCCATGACTCGCGGCCGGCCTGGCCTGGTTGTGGTTGTGGTTGTGG

VHH-R5: CATGCCATGACTCGCGGCCGGCCTGGCCCTTGCATACTTCATTCGTTCCTG

R1: CATGCCATGACTCGCGGCCGGCCTGGCCATGGGGGTCTTCGCTGTGGTGCG

137

138